ISSN NO. 2320-5407

Journal homepage: http://www.journalijar.com

INTERNATIONAL JOURNAL OF ADVANCED RESEARCH

RESEARCH ARTICLE

A comparative study of pure and Amaranth dye doped L-Alanine Thiourea single crystals

R. KANNAN, D. JAYARAMAN and S. ARAVINDHAN
Department of Physics Presidency College, Chennai-600005, Tamilnadu, India

Manuscript Info

Manuscript History:

Received: 18 March 2015
Final Accepted: 28 April 2015
Published Online: May 2015

Key words:

slow evaporation technique, NLO study, XRD study, dielectric properties

Corresponding Author

R. KANNAN

Abstract

Amaranth dye doped L-Alanine Thiourea single crystals were grown by slow evaporation technique with the vision to improve the properties of the crystal. The crystal structure of doped crystal was determined from Single crystal X-Ray diffraction and Powder X-Ray diffraction studies. The doping of the Amaranth dye in the grown crystal has been confirmed qualitatively by the FT-IR spectroscopy. The optical transparency of the crystals was identified from the UV-vis-NIR transmission spectrum. Thermo Gravimetric Analysis shows that the thermal stability of the crystal increases with dopant concentration. The doping of Amaranth dye increases the thermal stability, mechanical strength and laser damage threshold of the grown crystals compared to pure LATU crystals. The crystals were further subjected to other important characterizations such as dielectric measurement and NLO studies. The improvement in Second Harmonic Generation efficiency of doped crystal has also been reported.

Copy Right, IJAR, 2015,. All rights reserved

1. Introduction

Nonlinear optical (NLO) materials play a major role in nonlinear optics and in particular they have a great impact on information technology and industrial applications. In the last decade, however, this effort has also brought its fruits in applied aspects of nonlinear optics. This can be essentially traced to the improvement of the performances of the NLO materials. There has been a growing interest in crystal growth process, particularly, in view of the increasing demand for materials for technological applications (Laudise et al 1975, Brice 1986, Nalwa and Miyata 1996). The wide range of applicability of single crystals is evident in the fields of semiconductors, polarizers, infrared detectors, solid state lasers, nonlinear optic, piezoelectric, acousto-optic, photosensitive materials and crystalline thin films for microelectronics and computer industries. The growth of single crystals and their characterization towards device fabrication have assumed great impetus due to their significance in both academic research and applied research. Nonlinear optical (NLO) materials have a nonlinear response to the electric field associated with the light of a laser beam, leading to a variety of optical phenomena such as the generation of new light frequencies or the alteration of the material's optical properties. Organic nonlinear optical materials have been investigated due to their potentially high nonlinearities and rapid response in electro-optic effect compared to inorganic NLO materials. These molecular organic compounds with one or more aromatic systems in conjugated positions, leading to charge transfer systems have been intensely studied for the past two decades (Goto et al 1991). Considerable theoretical and experimental investigations have been done in order to understand the microscopic origin of nonlinear behaviour of organic NLO materials Kerkoc et al1990 and Dimitriev et al 1991. The conjugated πelectron system provides a pathway for the entire length of conjugation under the perturbation of an external electric field. Fictionalization of both ends of the πconjugated system with appropriate electron donor and acceptor groups can increase the asymmetric electronic distribution in either or both the ground and excited states, thus leading to an increased optical non-linearity (Prasad and Williams 1991). When acceptor and donor moieties are placed at terminal position of conjugated backbone, both linear and nonlinear optical properties have increased significantly which involves correlated and high

delocalized πelectron states. The magnitudes of molecular polarizability and hyperpolarizability coefficients are found to increase super linearly with an increase in conjugation length between the donor and the acceptor. The strength of donor and acceptor groups and order of their stacking along the backbone plays important roles in determining the magnitude of nonlinear optical (NLO) efficiency (Blanchard-Desce et al 1995). In case of organic crystals, two requirements are satisfied: (i) they are made of highly polarizable molecules, the so-called conjugated molecules, where highly delocalized p-electrons can easily move between electron donor and electron acceptor groups on opposite sides of the molecule, inducing a molecular charge transfer, (ii) the molecules are adequately packed to build up a noncentro symmetrical crystal structure that provides non vanishing second-order nonlinear coefficients (Chemla et al 1987 and Bosshard et al 1995). In parallel to the invention of new NLO materials, it is also important to modify the physical, optical and electrical properties of these materials either by adding functional groups [1] or incorporation of dopants [2,3] for tailor made applications. In the presence of dopants growth promoting factors like growth rate [4] and many of the useful physical properties like optical transparency [5,6] second harmonic generation (SHG) efficiency [3], laser damage threshold (LDT) etc. get enhance. The dopants or additives also influence the crystalline perfection which may in turn influence the physical properties depending on the degree of doping and as per the accommodating capability of the host crystal. Dye inclusion crystals are used for application of solid state lasers. The dye molecule is incorporated with the water soluble crystals and avoids many drawbacks like other solid materials such as working media for lasers. The dyes absorb in the visible range of 500–550 nm. Thus second harmonic generation of Nd-YAG laser light is suitable for pumping the dyes in order to achieve lasing effect [7]. Due to broad absorption in the visible region in the dye doped crystal it can be used as a filter. Amaranth dye is a synthetic acid dye containing both NN and CC chromophore groups (pyrazolone dye). It was made from amaranth plants. It is a red-brown dye; soluble in water; decomposes at 120 ˚C without melting; has been used in colouring food and in cosmetics. This anionic dye, which is stable and water soluble with an absorption peak at 520 nm, was chosen as a representative species for this study. To the best of our knowledge, there are no reports available on the influence of Amaranth dye on the growth and physical properties of L-Alanine Thiourea single crystals.

2. Experimental Procedure

L-Alanine Thiourea (LATU) was synthesized by dissolving high purity Thiourea and L-Alanine in the equimolar ratio in aqueous medium. Thiourea was first dissolved in Millipore water and then L-Alanine was added with continuous stirring for about 2 hours using a magnetic stirrer at 50 ˚C. The product was obtained as per the following reaction.

$$H_2N - CS - NH_2 + CH_3CHNH_2\,COOH \rightarrow H_2N - CS - NH_3^-CH_3CHNH_2COO^+$$

(Thiourea + L-Alanine → L-Alanine Thiourea)

The impurity content of L-Alanine Thiourea (LATU) was minimized by the process of recrystallization. The pH value of the solution was about 7.24. The pH value was adjusted to 3.5 by adding few drops concentrated hydrochloric acid [8]. Then it was filtered using Whatmann filter paper and the filtered solution was kept in a borosil beaker covered with an aluminium foil and the solvent was allowed to evaporate at room temperature. As a result of slow evaporation, after 30 days, colourless and transparent LATU crystal with dimensions of 12×3×3 mm^3 was obtained. The same experimental procedure was adopted for the synthesis of Amaranth dye (0.1 mol%) admixtured LATU salt. The seed crystal with perfect shape and free from macro defects was used for the growth of dye admixtured LATU crystal by slow evaporation method. The photographs of LATU and Amarnath dye admixtured LATU (AMLATU) crystals are shown in Fig. 1 and Fig. 2.

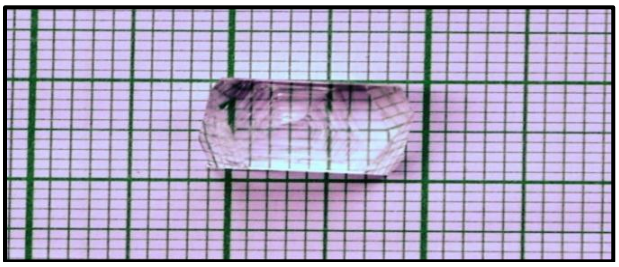

Figure 1. Grown LATU crystal

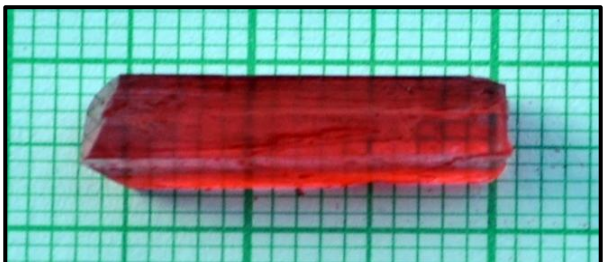

Figure 2. Grown AMLATU crystal

3. Result and discussion

3.1. Single crystal XRD analysis

The single crystal XRD analysis of LATU and Amaranth dye admixtured LATU(AMLATU) crystals were carried out using MESSRS ENRAF NONIUS CAD4-F, single X-ray diffractometer with MoKα (λ=0.71073 Å) radiation. The lattice parameters of LATU and AMLATU crystals obtained from single crystal XRD analysis are presented in Table 1.

Table 1. Comparison of lattice parameters of LATU and AMLATU.

S. No.	Crystal name	Axial lengths of unit cell (a, b and c)	Inter axial angles (α, β and γ)	Volume	Crystal system	Space group
01.	LATU	a = 9.6312 Å b = 5.6136 Å c = 9.4142 Å	α = γ = 90° β = 109.48°	508.98 $Å^3$	Monoclinic	$P2_1$
02.	AMLATU	a = 9.6811 Å b = 5.6251 Å c = 9.4011 Å	α = γ = 90° β = 109.48°	511.96 $Å^3$	Monoclinic	$P2_1$

The single crystal XRD study reveals that the presence of dopant has not altered the basic structure of the LATU crystal. The lattice parameter values of Amaranth dye admixtured crystal may be attributed to the lattice strain in the grown crystals due to the incorporation of the dye dopant.

3.2. Powder XRD Analysis

The grown crystals of LATU and AMLATU were crushed into fine powder and powder X-ray diffraction analysis has been carried out using Rich Seifert X-ray diffractometer. The X-axis of graph is 2θ. The Y-axis gives the intensity in arbitrary units. The samples were subjected to intense X-ray of wavelength 1.5406 Å (CuKα) at a scan speed of 1°/minute to obtain lattice parameters. The Miller indices (hkl), d-spacing and diffraction angle (2θ) are summarized for LATU and AMLATU are shown in Table 2 and Table 3 with the help of RexCell program and their powder diffractograms are shown in Fig. 3 & Fig. 4.

Table 2. Miller indices, d-spacing and 2θ-values of L-Alanine Thiourea (LATU) single crystal determined from powder XRD analysis using RexCell software.

S. No.	h	k	l	d(obs) (A°)	d(cal) (A°)	2θ (obs) (deg)	2θ (cal) (deg)
1	2	0	-1	4.59282	4.59479	19.303	19.294
2	1	0	-2	4.28883	4.28477	20.685	20.705
3	1	1	1	3.81913	3.81395	23.263	23.295
4	2	1	0	3.48218	3.48090	25.550	25.560
5	3	0	-1	3.13881	3.13725	28.401	28.415
6	2	1	-2	3.07372	3.07392	29.015	29.014
7	2	1	1	2.93698	2.93525	30.398	30.417
8	1	1	2	2.84657	2.84937	31.388	31.357
9	3	1	-1	2.73649	2.73839	32.685	32.662
10	3	0	1	2.52323	2.52358	35.536	35.531
11	1	2	1	2.46934	2.46928	36.338	36.339
12	0	2	2	2.31055	2.31088	38.933	38.927

Table 3. Miller indices, d-spacing and 2θ-values of Amaranth dye admixtured LATU single crystal determined from powder XRD analysis using RexCell software.

S. No.	h	k	l	d(obs) (A°)	d(cal) (A°)	2θ (obs) (deg)	2θ (cal) (deg)
1	1	1	1	4.58479	4.58976	19.337	19.316
2	2	0	-1	4.43740	4.43163	19.986	20.012
3	0	2	0	4.27487	4.27224	20.754	20.767
4	0	0	2	3.81086	3.80861	23.314	23.328
5	0	1	2	3.48218	3.47868	25.550	25.576
6	3	0	-1	3.14621	3.14441	28.333	28.349
7	2	1	-2	3.08081	3.07879	28.947	28.967
8	3	1	-1	2.94668	2.95093	30.296	30.251
9	0	2	2	2.84657	2.84293	31.388	31.429
10	3	0	1	2.73649	2.73578	32.685	32.694
11	1	3	1	2.52323	2.52339	35.536	35.534
12	1	1	-3	2.46934	2.47157	36.338	36.304
13	4	1	-1	2.31055	2.31056	38.933	38.933

From the X-ray powder diffraction data, the lattice parameters for AMLATU were found to be a = 9.6711 Å, b = 5.6391 Å and c = 9.4199 Å. This is in close agreement with the values obtained from single crystal X-ray diffraction analysis for AMLATU.

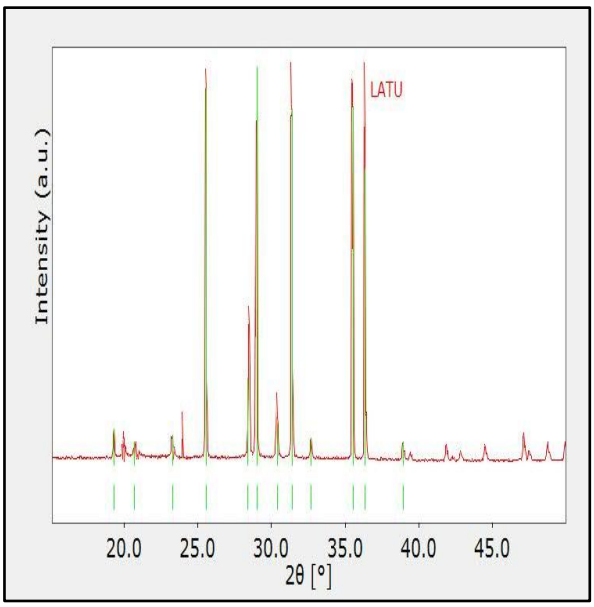

Figure 3. PWXRD spectrum of LATU crystal

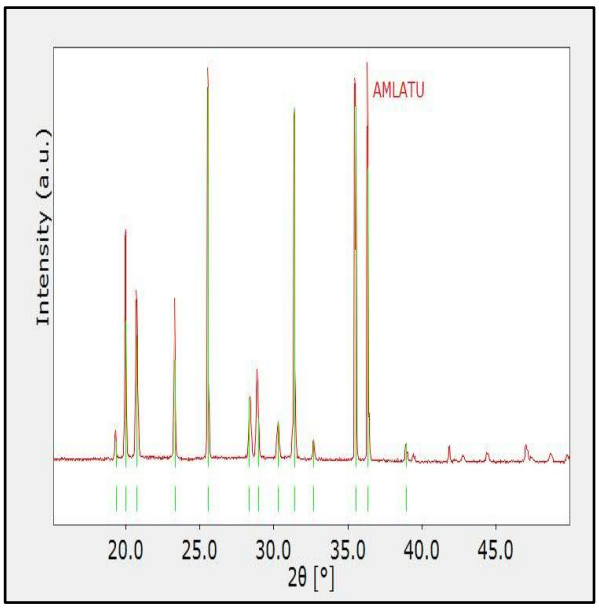

Figure 4. PWXRD spectrum of AMLATU crystal

The change in intensity of peaks as well as addition in number of peaks for AMLATU in the powder X-ray diffraction pattern reveal that the dye doped crystal is slightly distorted compared to the pure LATU. This may be attributed to strains on the lattice by the absorption or substitution of Amaranth dye in LATU crystal.

3.3. High resolution X-ray diffraction studies

The crystalline perfection of the grown crystals were characterized by HRXRD analysis by employing a multicrystal X-ray diffractometer with MoKα_1 radiation designed and developed at National Physical Laboratory (NPL) New Delhi [9] has been used to record high-resolution diffraction curves (DCs). The well-collimated and monochromated MoKα_1 beam obtained from the three monochromator Si crystals set in dispersive (+,-,-) configuration has been used as the exploring X-ray beam. The specimen crystal is aligned in the (+,- ,-,+) configuration. Due to dispersive configuration, though the lattice constant of the monochromator crystal(s) and the specimen are different, the unwanted dispersion broadening in the diffraction curve (DC) of the specimen crystal is insignificant. Before recording the diffraction curve, to remove the non-crystallized solute atoms remained on the surface of the crystal and also to ensure the surface planarity, the pure LATU and Amaranth dye admixtured LATU crystals were first lapped and chemically etched in a non-referential etchant of water and acetone mixture in 1:2 ratios. Fig. 5 and Fig. 6 show the high-resolution diffraction curves (DCs) recorded for pure LATU and Amaranth dye admixtured LATU crystals using (3 0 0) diffracting planes in symmetrical Bragg geometry by employing the multicrystal X-ray diffractometer with MoKα_1 radiation.

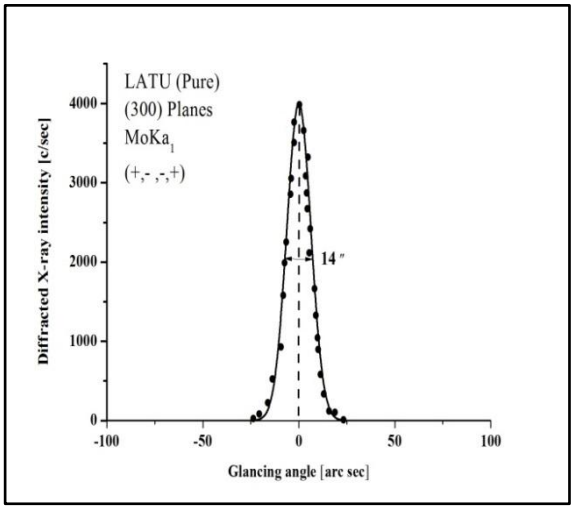

Figure 5. HRXRD curve of pure LATU crystal

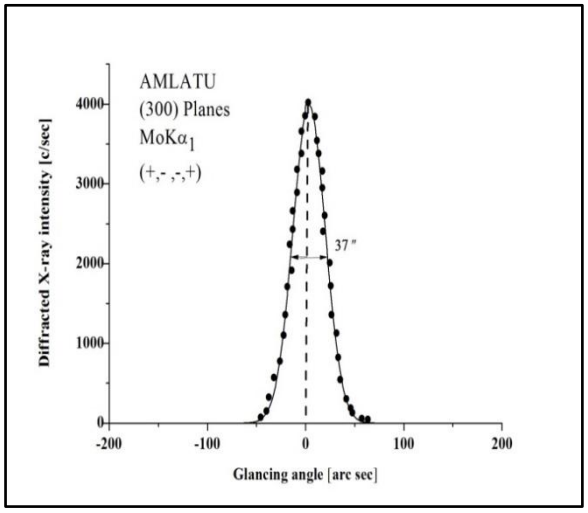

Figure 6. HRXRD curve of AMLATU crystal

The curves are very sharp having full width at half maximum (FWHM) of 14 arc sec for pure LATU and 37 arc sec for Amaranth dye admixtured LATU crystals as expected for nearly perfect crystals from the plane wave dynamical theory of X-ray diffraction [10]. The absence of additional peaks and the very sharp DC shows that the crystalline perfection of the specimen crystals is extremely good without having any internal structural grain boundaries and mosaic nature. The increase in FWHM without having any additional peaks in DC of Amaranth dye doped LATU crystal indicates the incorporation of Amaranth dye in the crystalline matrix of LATU crystal. In DC of Amaranth dye doped LATU crystal, for a particular angular deviation ($\Delta\theta$) of glancing angle (θ) with respect to the Bragg peak position (taken as zero for the sake of convenience), the scattered intensity is much more in the positive direction in comparison to that of the negative direction. This feature or asymmetry in the scattered intensity clearly indicates that the Amaranth dopants predominantly occupy the interstitial positions in the lattice and elucidates the ability of accommodation of dopants in the crystalline matrix of the LATU crystal. This can be well understood by the fact that due to incorporation of dopants in the interstitial positions, the lattice around the dopants compresses and the lattice parameter d (interplanar spacing) decreases and leads to give more scattered (also known as diffuse X-ray scattering) intensity at slightly higher Bragg angles(θ_B) as d and sin θ_B are inversely proportional to each other in the Bragg equation ($2d \sin \theta_B = n\lambda$; n and λ being the order of reflection and wavelength respectively which are fixed). It may be mentioned here that the variation in lattice parameter is only confined very close to the defect core which gives only the scattered intensity close to the Bragg peak. Long range order could not be expected and hence change in the lattice parameter is also not expected [11]. The HRXRD results confirm an important finding that Amaranth dye entrapped in the LATU crystals, but the amount is limited to a critical value and above which the crystals have a tendency to develop structural grain boundaries [12].

3.4. Fourier Transform Infrared Spectroscopy

The mid Fourier transform infrared spectrum of pure and dye doped LATU crystals were recorded at 300 K in the range of 4000–400 cm^{-1} using the KBr pellet technique. The FTIR spectra of pure and dye admixtured LATU crystals are shown in Fig. 7 and Fig. 8. The incorporation of Amaranth dye in LATU crystal has been strongly verified by spectral analysis. The absorptions at 3796, 3560 and 3373 cm^{-1} in the Amarnath dye doped LATU crystals may be attributed to hydrogen bonded OH stretching. The NH^{+3} asymmetric bending and CH_2 stretching vibrations occur at 3181 cm^{-1} and at 2809 cm^{-1}. The asymmetric stretching vibration of CO_2 is observed at 1558 cm^{-1}. In the Amaranth dye LATU spectrum, the OH stretching in the high energy region is very much broadened, due to hydrogen bonding. The peak at 511 cm^{-1} is due to C=S stretching vibration. The aliphatic C-H stretching mode at 2736 cm^{-1} confirms the presence of Amaranth dye in LATU. The narrow bands at 737, 632 and 511 cm^{-1} are observed in Amaranth dye added as compared to LATU. The vibration frequencies of L-Alanine Thiourea are compared with Amaranth dye admixtured L-Alanine Thiourea in Table 4 to confirm the incorporation of Amaranth dye in LATU crystal.

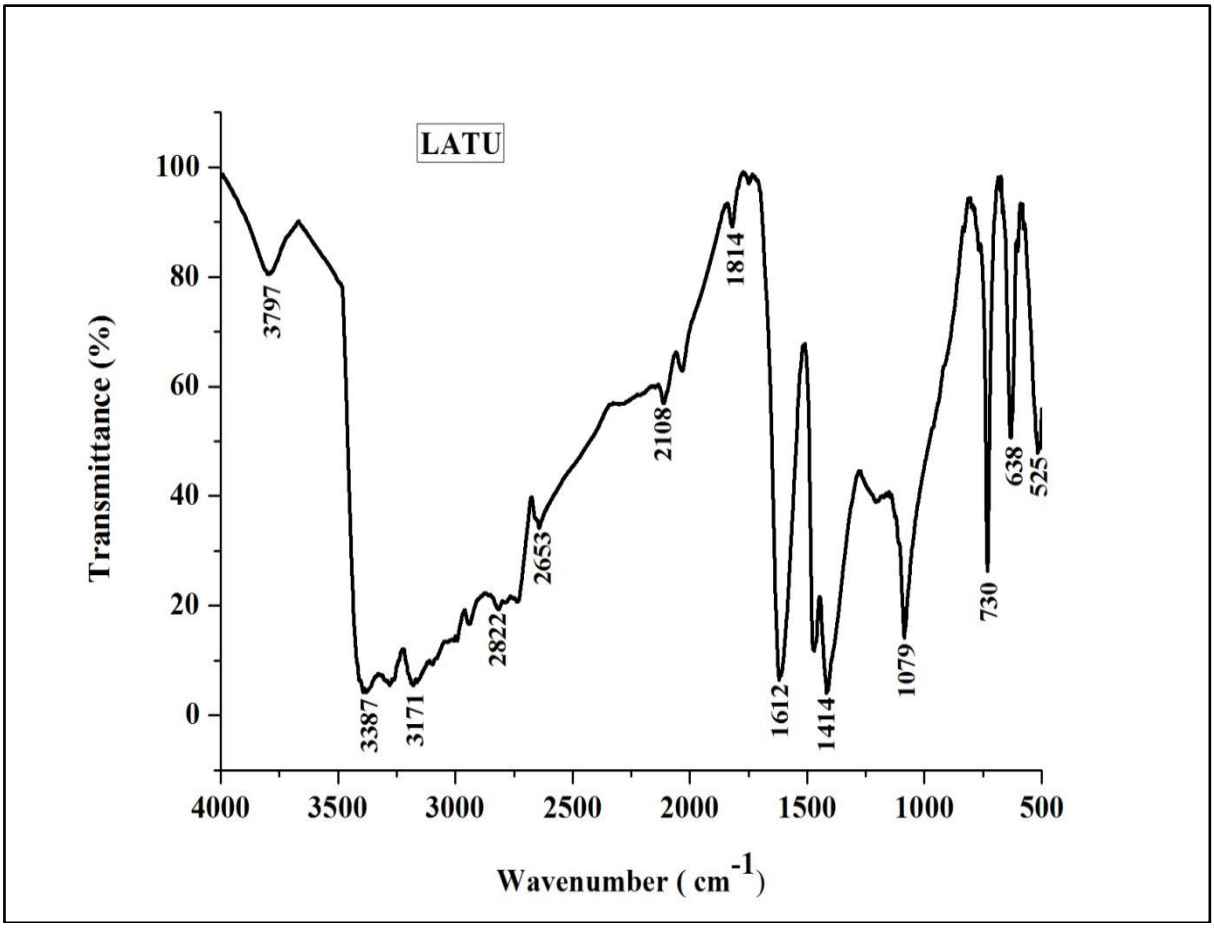

Figure 7. FTIR spectrum of grown L-Alanine Thiourea (LATU) single crystal.

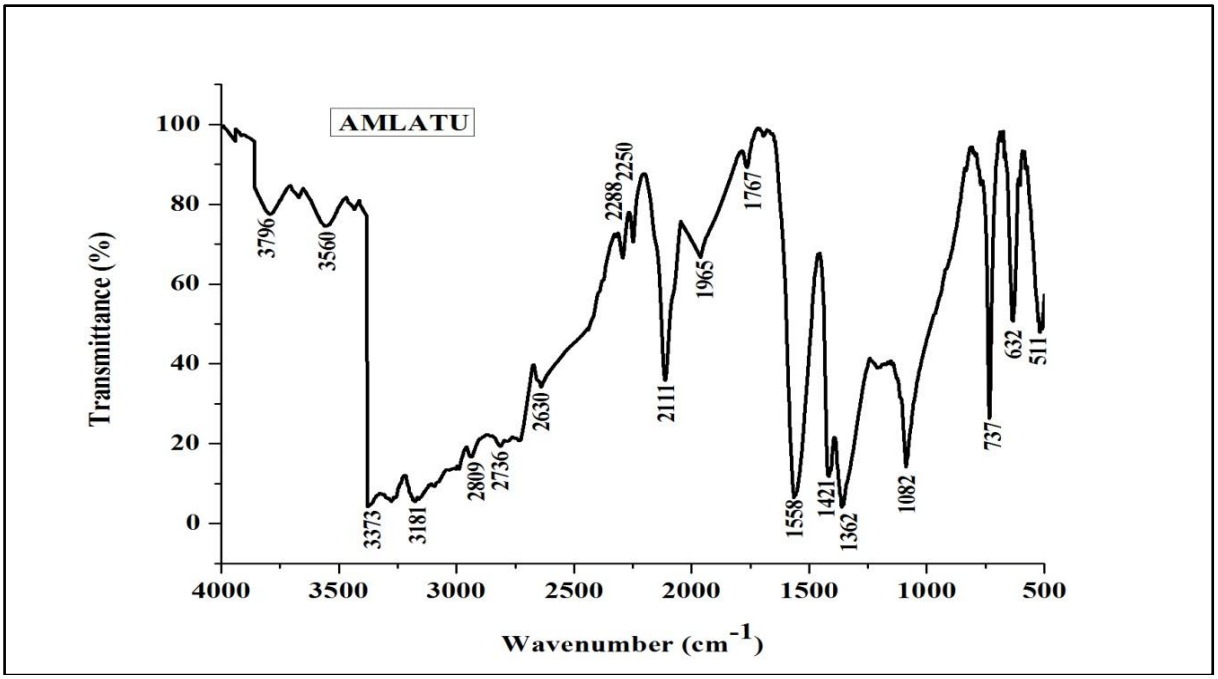

Figure 8. FTIR spectrum of grown Amaranth dye admixtured LATU single crystal.

Table 4. Infrared absorption frequencies (cm^{-1}) of L-Alanine Thiourea (LATU) and Amaranth dye admixtured LATU (AMLATU) crystals

S.No.	L-Alanine Thiourea (LATU)	Amaranth dye admixtured LATU (AMLATU)	Assignment
1	3797	3796, 3560, 3373	OH- stretching
2	3171	3181	NH_3^+ symmetric stretching
3	2822	2809	$=CH_2$ stretching
4	-	2736	Aliphatic (C-H) stretch
5	2653	2630	C-H symmetric stretching
6	2108	2111	Over tone region with a combination of symmetric NH_3^+ bending and torsional vibrations
7	1814	1965	C=O absorption
8	1612	1767	Asymmetric bending of NH_3^+ and C=N stretching
9	-	1558	CO_2 asymmetric stretching
10	1414	1421	C= O stretching
11	1079	1082	Symmetrical C-O-C stretching
12	730	632	C-H in plane bending
13	638	511	C=S stretching

3.5. UV-visible spectral study

The UV-visible spectra of pure and Amaranth dye admixtured analyses have been carried out using Shimadzu UV-vishible spectrophotometer in the wavelength range of 100-1100 nm. Transmission spectra are very important

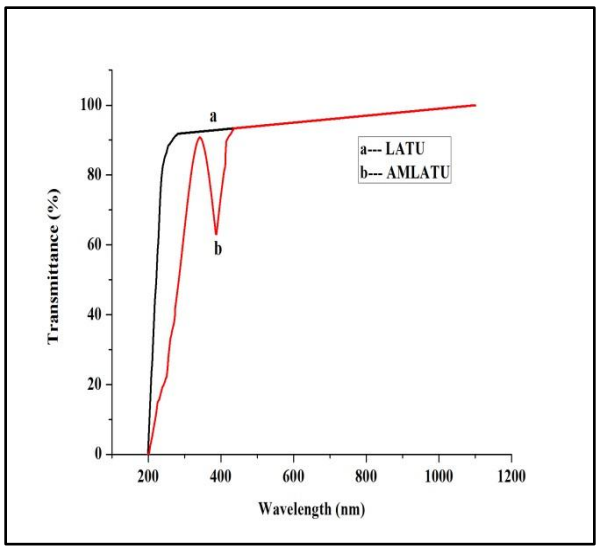

Figure 9. UV-vis-NIR transmission spectra for LATU and AMLATU crystals

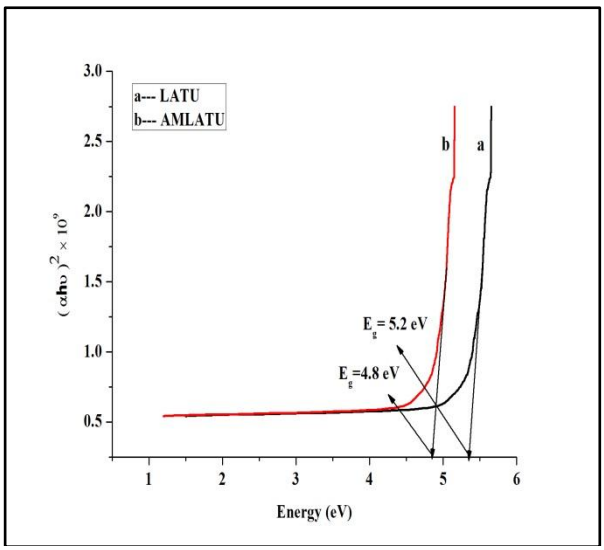

Figure 10. Photon energy vs $(\alpha h\upsilon)^2$ for LATU and AMLATU crystals

for any NLO material because a nonlinear optical material can be of practical use only if it has wide transparency window [13]. The UV-vis spectra of LATU and AMLATU are shown in Fig. 9. In the case of pure percent transmittance is occurred at 385.93 nm. LATU, a sharp fall in percent transmittance is occurred at 209 nm. For AM dye admixtured LATU, the fall in Such variation in percent transmittance is due to electronic excitation of AM dye doped LATU crystal. The good transparency with lower cut off wavelength at 385.93 nm makes the AMLATU crystal useful for optoelectronics applications.

3.6 Optical band gap energy (E_g) calculation

The band gap energy of the pure and Amaranth dye admixtured LATU crystals were calculated from the Fig. 10 by taking Photon energy ($h\upsilon$) values along X-axis and $(\alpha h\upsilon)^2$ values along Y-axis for LATU and AMLATU crystals. The optical absorption coefficient (α) was calculated using the relation

$$\alpha = (2.3026 * \log (1/T)) / t \quad (1)$$

where T is the transmittance and t is the thickness of the crystal. The band gap energy values were calculated by extrapolation of the linear part of the curve for LATU and AMLATU and found to be 5.2 eV and 4.8 eV respectively. The decrease in band gap energy value of dye admixtured LATU may be due to incorporation of dye in the LATU crystal lattices. The value of band gap energy for AMLATU crystal suggests that the material is dielectric in nature to possess wide transmission range. The large transmission in the entire visible region and lower cut off wavelength enable it to be a potential material for second and third harmonic generation [14].

3.7. Thermo gravimetric analysis (TGA)

Thermo Gravimetric Analysis (TGA) and Differential Thermal Analysis (DTA) were carried out for LATU and AMLATU crystals using TA Q-500 analyser. TGA and DTA curves for pure and Amaranth dye admixtured LATU are shown in Fig. 11 and Fig. 12. The powder samples were used for the analysis in the temperature range of 0 ˚C to 1000 ˚C at a heating rate of 10 ˚C/min in the nitrogen atmosphere. In pure LATU, the major weight loss occurs between 173.53 ˚C and 241.19 ˚C. The change in weight loss confirms the decomposition nature of the sample. Differential thermal analysis confirms through a sharp endothermic peak at 217.56 ˚C revealing the major weight loss. Further, degradation of the sample takes place from 274 ˚C to 760 ˚C where the loss of weight is about 5.41% due to liberation of volatile substances like sulfur oxide and amino acid L-Alanine [15]. The weight loss of 2.976% at the end is due to the release of CO molecules. Hence, it is concluded that the grown material is thermally stable up to 173.53 ˚C.

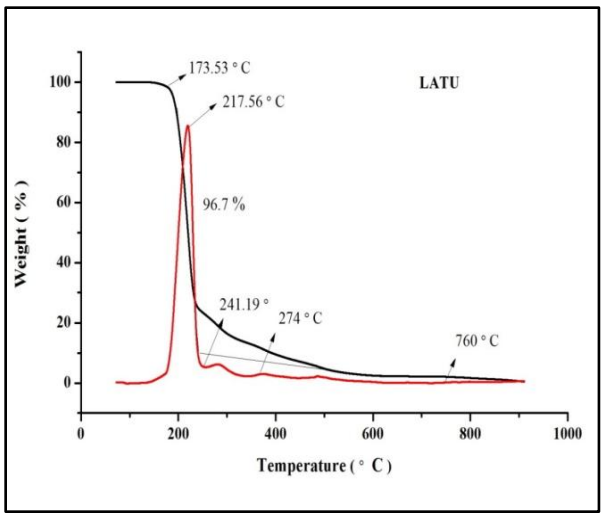

Figure 11. TGA and DTA curves of LATU crystal

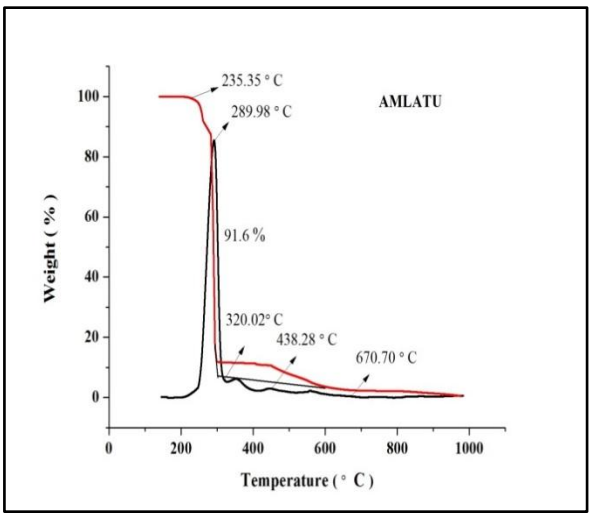

Figure 12. TGA and DTA curves of AMLATU crystal

In Amaranth dye admixtured LATU crystal, the major weight loss occurs between 235.35 ˚C and 320.02 ˚C. The change in weight loss confirms the decomposition nature of the sample. Differential thermal analysis confirms through a sharp endothermic peak at 289.98 ˚C revealing the major weight loss. Further, degradation of the sample takes place from 438.28 ˚C to 670.70 ˚C where the loss of weight is about 2.01 % due to absorption of energy for breaking of bonds during the decomposition of the compound. Hence, it is concluded that the Amaranth dye admixtured LATU crystal is suitable for optoelectronics applications up to 235.35 ˚C.

3.8. Dielectric Analysis

The dielectric studies of pure LATU and Amaranth dye admixtured LATU crystals were carried out using the HIOKI 3532-50 LCR HITESTER instrument. The capacitance values for LATU and AMLATU crystals were determined for frequencies varying from 50 Hz to 5 MHz at room temperature. The variations of dielectric constant and dielectric loss as a function of log frequency are shown in Fig. 13 and Fig. 14.

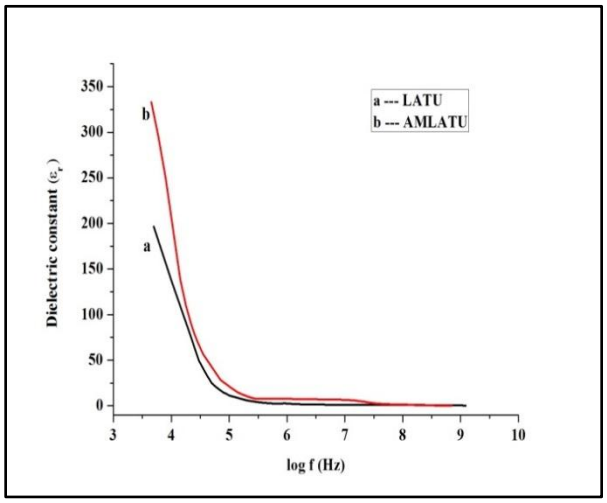

Figure 13. Variation of dielectric constant of pure LATU and AMLATU

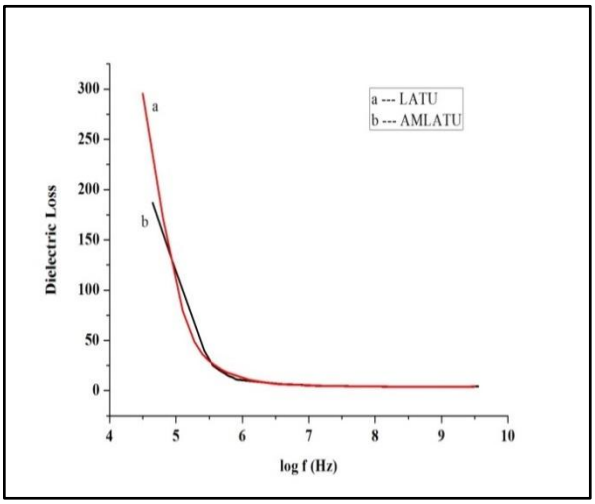

Figure 14. Variation of dielectric loss of pure LATU and AMLATU

It is observed that the dielectric constant of pure LATU is 196 where 333 for Amaranth dye admixtured LATU crystal. The high value of dielectric constant at low frequencies may be due to incorporation of Amaranth dye in LATU in the grown crystal and better orientation of dipoles in the molecules of the crystals. The low value of

dielectric loss indicates that the pure and Amaranth dye admixtured LATU crystals have lesser defects, which is a desirable property for NLO applications.

3.9. Microhardness Measurements

Microhardness behaviour of pure LATU and AMLATU single crystals were tested by using Shimadzu make-model-HMV-2 fitted with Vickers pyramidal indenter and attached to an incident light microscope. The indentations were made on the flat surface with the load ranging from 25 to 100 g and the indentation time was kept as 10s for all the loads. The Vickers hardness number H_v was calculated from the following expression,

$$H_V = ((1.8544*P)) / d^2 \quad kg / mm^2 \qquad (2)$$

where P is the applied load in kg, d is the diagonal length of the indentation impression in mm and 1.8544 is a constant of a geometrical factor for the diamond pyramid. Vickers hardness number was calculated and a graph has been plotted between the hardness values and the corresponding loads for the crystals as shown in Fig. 15. From the results, it is observed that the hardness number decreases with increasing load up to 75 g and attains saturation for further increase in load. Beyond this load cracks were found both in pure LATU and AMLATU single crystals. From the Fig. 15, it is observed that the microhardness value of dye admixtured crystal is slightly higher than that of the pure LATU and it is due to the presence of organic Amaranth dye molecule in the interstitial sites of pure LATU crystal.

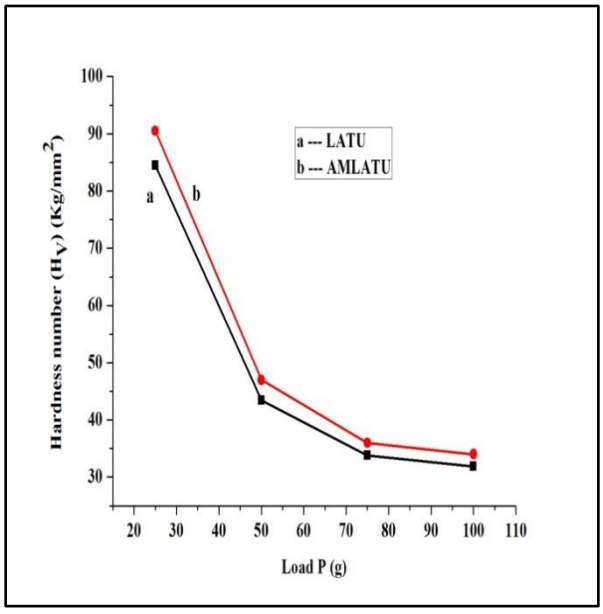

Figure 15. Variation of hardness with applied load for LATU and AMLATU single crystals

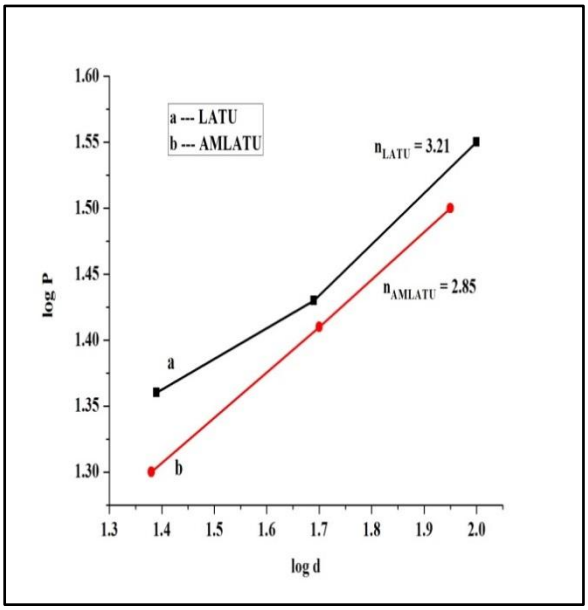

Figure 16. Variation of log (P) with log (d) for LATU and AMLATU single crystals

The Mayer's index number was calculated from the Mayer's law, which relates the applied load(P) and indentation diagonal length(d).

$$P = ad^n \qquad (3)$$

where 'a' is the material constant and 'n' is the Mayer's index or work hardening coefficient. The values of the work hardening coefficient (n) were estimated from the plot of log P versus log d drawn by the least square fit method and it is shown in Fig. 16. The work hardening coefficients (n) for pure LATU and Amaranth dye admixtured LATU crystals were found to be 3.21 and 2.85 respectively. Onitsch [16] pointed out that 'n' lies between 1 and 1.6 for moderately hard materials and it is more than 1.6 for soft materials. The observed values of Mayer's index for LATU and AMLATU are 3.21 and 2.85 and hence they belong to the soft materials category.

3.10. Laser damage threshold studies

The laser damage density is one of the important parameters that decide the applicability of the material for high power laser applications. The laser damage threshold values were measured using a Q-switched Nd-YAG laser source of pulse width 10ns and 10Hz repetition rate operating in TEM00 mode. The energy per pulse of 532nm laser radiation attenuated using appropriate neutral density filters was measured using an energy meter (Coherent EPM 200) which is externally triggered by the Nd:YAG laser. If the material has a low damage threshold, it severely limits its application, though it may have excellent properties like high optical transmittance and high SHG efficiency [17]. For surface damage, the sample was placed at the focus of a plano-convex lens of focal length 30 cm. The (100) plane of pure and dye admixtured crystals was used for the laser damage studies. The surface threshold of the crystal was calculated using the expression:

$$\textbf{Power density (Pd)} = E/\tau\pi r^2 \qquad (4)$$

Where E is the energy (mJ), τ is the pulse width(ns) and r is the radius of the spot (mm). The measured multiple shot (150 pulses) laser damage threshold values of pure and dye admixtured LATU crystals are 9 and 8.1 GW/cm^2 respectively. The decrease in laser damage threshold value of dye admixtured LATU may be due to incorporation of dye in the LATU crystals

3.11. NLO Studies

Nonlinear optical (NLO) property of pure L-Alanine Thiourea (LATU) and Amaranth dye admixtured LATU crystals were determined by Kurtz powder technique using the Nd:YAG Q-switched laser beam. The samples of same sizes were illuminated using Q-switched, mode locked Nd:YAG laser with input pulse of 6.2 mJ. The second harmonic signals of 384 mV and 690 mV were obtained for pure and Amaranth dye admixtured LATU crystals with reference to KDP (275 mV). Thus, the SHG efficiency of LATU and Amaranth dye admixtured LATU crystals was found to be 1.39 and 2.5 times greater than the standard KDP crystal. The relative SHG efficiency of xylenol admixtured LATU crystal was found to be 1.79 times higher than that of pure LATU crystal.

4. Conclusion

Good quality of LATU and Amaranth dye admixtured LATU crystals were grown by slow evaporation method. The unit cell parameters of the crystals obtained from single crystal XRD showed that the LATU and AMLATU crystals belong to monoclinic system with space group $P2_1$. Sharp peaks of powder XRD pattern of the crystals confirm the good crystalline nature of the grown crystals and the incorporation of Amaranth dye into LATU crystal lattice. The functional groups of AMLATU crystal were identified by FTIR spectral analysis and they have confirmed the presence of organic additive Amaranth dye in LATU crystal. The UV-vis-NIR transmittance spectra showed that the crystals had a wide optical window and the absorption due to Amaranth dye in LATU crystal. The addition of Amaranth dye in LATU crystal increased the thermal stability of pure LATU crystal. The sharpness of the endothermic peak shows good degree of crystallinity of the crystal. The Vickers micro hardness values were calculated in order to understand the mechanical stability of the crystals. Dielectric studies for the crystal were studied. NLO studies have confirmed that the SHG efficiency value was significantly enhanced due to the presence of Amaranth dye in LATU crystal.

Acknowledgments

The authors are very much thankful to Prof. P.K. Das, IPC Department, IISc, Bangalore for extending laser facilities to measure SHG efficiency and to SAIF, IIT Madras Chennai for providing the single crystal XRD, powder crystal XRD, thermal studies and UV–studies.

References

[1] Sweta Moitra and Tanusree Kar, (2007), Opt. Mater., vol. 30, 508.

[2] Zernike, F. and Midwinter, J.E., (1973), Applied nonlinear optics, Wiley, New York.

[3] Bhagavannarayana, G., Parthiban, S. and Meenakshisundaram, S., (2008), Cryst. Growth Des., vol. 8, 446.

[4] Vries de, S.A., Goedtkindt, P., Bennett, S.L., Huisman, W.J., Zwanenburg, M.J., Smilgies, D.M., De Yoreo, J.J., Enckevort van, W.J.P., Bennema, W.P. and Vlieg, E., (1998), Phys. Rev. Lett., vol. 80, 2229.

[5] Kar, S., Bhatt, R., Bartwal, K. S. and Wadhawan, V.K., (2004), Cryst. Res. Technol., vol. 39, 230.

[6] Winkler, E., Etchegoin, P., Fainstein, A. and Fainstein, C., (2000), Phys. Rev., B 61, 15756.

[7] Pritula, I., Gayvoronsky, V., Gromov, Yu., Kopylovsky, M., Kolybaeva, M., Puzikov, V., Kosinova, A., Savvin, Yu., Velikhov, A., Levchenko, (2009), Opt. Commun., 282, 1141.

[8] Palanisamy, S., Balasundaram, O.N., (2008), Growth, Optical and Mechanical Properties of Alanine Sodium Nitrate (ASN), Rasayan Journal of Chemistry, vol. 1, pp. 782-787.

[9] Lal, K. and Bhagavannarayana, G., (1989), "A high-resolution diffuse X-ray scattering study of defects in dislocation-free silicon crystals grown by the float-zone method and comparison with Czochralski-grown crystals", J. Applied Crystallography, vol. 22, 209-215.

[10] Batterman, B.W., Cole. H., (1964), Dynamic diffraction of X-rays by perfect crystals, Rev. Mod. Phys., vol. 36, pp. 681-717.

[11] Bhagavannarayana, G., Kushwaha, S.K., Shakir, M. and Maurya, K.K., (2010), J. Appl. Crystallogr., vol. 44, pp. 122-128.

[12] Bhagavannarayana, G. and Kushwaha, S.K., (2010), Enhancement of SHG efficiency by urea doping in ZTS single crystals and its correlation with crystalline perfection as revealed by Kurtz powder and high-resolution X-ray diffraction methods, J. Appl. Crystallogr., vol. 43, pp. 154-162.

[13] Anandan, P., Jayavel, R., Saravanan, T., Parthipan, G., Vedhi, C. and Mohan Kumar, R., (2012), "Crystal growth and characterization of L-histidine hydrochloride monohydrate semiorganic nonlinear optical single crystals", Optical Materials, vol. 30, pp. 1225-1230.

[14] Ramajothi, J. and Dhanuskodi, S., (2007), "Crystal growth, thermal and optical studies on a semiorganic nonlinear optical material for blue-green laser generation", Spectrochimica Acta part A, vol. 68, pp. 1213-1219.

[15] Dhumane, N.R., Hussaini, S.S., Kunal datta, Prasanta ghosh and Mahendra, Shirsat, D., (2010), J. Pure Appl. & Ind. Phys., vol. 1, pp. 45-52.

[16] Onitsch, E.M., (1956), "The present status of testing the hardness of materials", Mikroskopie., vol. 95, pp. 12-14.

[17] Nakatani, H., Bosenberg, W.R., Cheng, L.K., Tang, C.L., (1988), Appl. Phys. Lett., vol. 53, 2587–2589.